The High Time Resolution Universe Pulsar Survey I: System configuration and initial discoveries

M. J. Keith[1]⋆, A. Jameson[2], W. van Straten[2], M. Bailes[2], S. Johnston[1], M. Kramer[3,4],
A. Possenti[5], S. D. Bates[4], N. D. R. Bhat[2], M. Burgay[5], S. Burke-Spolaor[2,1],
N. D'Amico[5], L. Levin[2,1], P. L. McMahon6, 7, S. Milia[5,8], B. W. Stappers[4]

[1] *Australia Telescope National Facility, CSIRO, P.O. Box 76, Epping, NSW 1710, Australia*
[2] *Swinburne University of Technology, Centre for Astrophysics and Supercomputing Mail H39, PO Box 218, VIC 3122, Australia*
[3] *Max Planck Institut für Radioastronomie, Auf dem Hügel 69, 53121 Bonn, Germany*
[4] *University of Manchester, Jodrell Bank Centre for Astrophysics, Alan Turing Building, Manchester M13 9PL, UK*
[5] *INAF-Osservatorio Astronomico di Cagliari, località Poggio dei Pini, strada 54, I-09012 Capoterra, Italy*
[6] *Berkeley Wireless Research Center, University of California, Berkeley, CA 94704, USA*
[7] *Department of Electrical Engineering, University of Cape Town, Rondebosch, 7701, South Africa*
[8] *Dipartimento di Fisica, Università degli Studi di Cagliari, Cittadella Universitaria, 09042 Monserrato (CA), Italy*

ABSTRACT

We have embarked on a survey for pulsars and fast transients using the 13-beam Multibeam receiver on the Parkes radio telescope. Installation of a digital backend allows us to record 400 MHz of bandwidth for each beam, split into 1024 channels and sampled every 64 μs. Limits of the receiver package restrict us to a 340 MHz observing band centred at 1352 MHz. The factor of eight improvement in frequency resolution over previous multibeam surveys allows us to probe deeper into the Galactic plane for short duration signals such as the pulses from millisecond pulsars. We plan to survey the entire southern sky in 42641 pointings, split into low, mid and high Galactic latitude regions, with integration times of 4200, 540 and 270 s respectively. Simulations suggest that we will discover 400 pulsars, of which 75 will be millisecond pulsars. With $\sim 30\%$ of the mid-latitude survey complete, we have re-detected 223 previously known pulsars and discovered 27 pulsars, 5 of which are millisecond pulsars. The newly discovered millisecond pulsars tend to have larger dispersion measures than those discovered in previous surveys, as expected from the improved time and frequency resolution of our instrument.

Key words: pulsars: general

1 INTRODUCTION

Pulsars are fascinating celestial objects, with spin periods ranging from ~ 1.6 ms to ~ 8.5 s and magnetic fields that span more than five orders of magnitude. Their study yields a better understanding of a variety of physics problems, from acceleration of particles in the ultra-strong magnetic field, to tests of gravity in the strong field regime. Pulsars provide useful probes of their environments whether inside pulsar wind nebulae, the centres of globular clusters or the Galactic Centre. Discovery of these unique objects has continued unabated for more than 40 years, and the diversity in their properties means that, even though nearly 2000 pulsars,

including ~ 170 millisecond pulsars (MSPs), are currently known, further discoveries are warranted.

In the past decade alone, surveys have uncovered a number of intriguing objects. These include the pulsar with the fastest rotation period (in the globular cluster Terzan 5; Hessels et al. 2006), the double pulsar system (Burgay et al. 2003; Lyne et al. 2004) and its impressive tests of general relativity (Kramer et al. 2006), the 'missing link' between the low-mass X-ray binaries and the MSPs (Archibald et al. 2009), rotating radio transients (McLaughlin et al. 2006), and young, energetic pulsars such as PSR J1028–5819 (Keith et al. 2008) with their subsequent tie to gamma-ray pulsars and their emission properties (Weltevrede et al. 2010). Furthermore, timing of MSPs provides highly accurate parameters (Verbiest et al. 2009) possibly leading to the detection of gravitational waves in the near future

(Hobbs et al. 2009). Finally, the discovery of a burst of radio emission of unknown origin but seemingly at cosmologically distances (Lorimer et al. 2007) has motivated searches for other such events.

Since the discovery of pulsars (Hewish et al. 1968), searches have been split into targeted and untargeted surveys. Targets of interest include, for example, globular clusters, supernova remnants, the Galactic Centre, and other regions known to be rich in pulsars. Although targeted searches are highly efficient in their use of telescope time, it is impossible to predict the location of the majority of pulsars. Therefore, untargeted searches over large areas of sky are the only way to significantly increase the number of known pulsars.

Since the early 1990s, large-area pulsar surveys with the Parkes telescope, such as the low frequency Parkes Southern Pulsar Survey (PSPS; Manchester et al. 1996) and the higher frequency Parkes Multibeam Pulsar Survey (PMPS; Manchester et al. 2001), Swinburne Intermediate Latitude Survey (SILS; Edwards et al. 2001) and its extensions (Jacoby et al. 2009) have led to the discovery of nearly 1000 pulsars. The all-sky PSPS was highly successful in finding MSPs (Lyne et al. 1998), but the low observing frequency limited the survey volume, especially towards the Galactic plane. The success of the later surveys was due to a combination of the higher observing frequency, the low system temperature and the large field of view provided by the 13-beam 'Multibeam' receiver (Staveley-Smith et al. 1996). These surveys had relatively coarse frequency resolution however, and this limited the searchable volume for short duration pulses from MSPs and/or transient bursts. For the PMPS this limit was due to the costs associated with replicating complex sets of analogue filters over 13 beams and the processing power available in the late 1990s.

In the 14 years since the commissioning of the Multibeam receiver, there has been a great advance in the development of backend recording technology. As pen chart recorders gave way to digital data analysis in the early 1970s, so analogue signal processing equipment is now being replaced by digital systems that offer a more affordable way to obtain higher time and frequency resolution. Increased frequency resolution allows for better correction of the dispersive effects of the interstellar medium, which, in combination with the higher time resolution, gives increased sensitivity to short duration pulses, such as those from MSPs.

Encouraged by these developments, we conceived the 'High Time Resolution Universe' (HTRU) survey, motivated by two main drivers: to increase our understanding of the population of MSPs and to characterise the transient sky on timescales down to tens of microseconds. These drivers led us to build a new digital backend system connected to the Parkes Multibeam receiver. We use this new backend to give the HTRU survey four times the time resolution and eight times the frequency resolution of the PMPS. This allows us to detect MSPs for which interstellar dispersion had hidden from previous surveys (Bates et al. in prep). With the discovery of the radio magnetar PSR J1622–4950 (Levin et al. 2010), we have also shown that the transient nature of some exotic pulsars gives us good reason to re-survey areas of sky that are already well studied.

The HTRU survey intends to be an all sky survey for pulsars and short duration radio transients, with a strong

Table 1. Survey parameters for the three parts of the HTRU survey.

Survey	High	Mid	Low
Region	$\delta < +10°$	$-120° < l$ $l < 30°$ $|b| < 15°$	$-80° < l$ $l < 30°$ $|b| < 3.5°$
$\tau_{\rm obs}$ (s)	270	540	4300
$N_{\rm beams}$	443287	95056	15990
$\tau_{\rm samp}$ (μs)	64	64	64
B (MHz)	340	340	340
$\Delta\nu_{\rm chan}$ (kHz)	390.625	390.625	390.625
$N_{\rm chans}$	870	870	870
Data length (samples)	$\sim 2^{22}$	$\sim 2^{23}$	$\sim 2^{26}$
Data/beam (GB)	1.0	2.0	16.0
Data/total (TB)	435	190	250

focus on the lower Galactic latitudes, where we make most use of the higher frequency resolution for negation of interstellar dispersion. A parallel effort is taking place at the Effelsberg radio telescope, covering the northern sky to a similar sensitivity, so as to provide a true all-sky survey at high time resolution.

In Section 2 of this paper we describe the survey strategy and the predicted results. Section 3 outlines the observing setup in hardware and software. Section 4 describes the analysis software that is being used to process the survey data. In Section 5 we compute and measure the effective sensitivity limits of the survey. Finally, in Section 6 we give the basic parameters of the first pulsars discovered in the HTRU survey.

2   SIMULATION AND SURVEY STRATEGY

The HTRU survey of the southern sky is composed of three parts, outlined in Table 1. Other than the observation time and sky coverage, the observing parameters are identical for all three parts. The **low-latitude** component covers a thin strip of the Galactic plane, with Galactic latitude $|b| < 3.5°$ and longitude $-80° < l < 30°$. The 4200 s observation time is twice that of the PMPS, providing the most thorough survey of the inner Galactic plane to date. The **mid-latitude** component covers $|b| < 15°$ and $-120° < l < 30°$. Here the observation time is 540 s, allowing for a large area of sky to be covered quickly. Finally, the **high-latitude** component covers the entire sky south of declination $+10°$ with 270 s integrations, excluding the region covered by the mid-latitude survey. Broadly speaking, the aims of the low-latitude part is to discover faint pulsars deep in the Galactic plane, whereas the mid-latitude survey will find bright MSPs suitable for timing array projects. Finally, the high-latitude survey will give us a snapshot of the transient sky at 64 μs resolution.

Detection of MSPs is limited by a combination of dispersion measure (DM) broadening in individual frequency channels, scattering in the interstellar medium and luminosity. For sufficiently luminous MSPs, the PMPS was predominantly limited by dispersion broadening in the 3 MHz channels, rather than by scattering. The increased frequency resolution of the HTRU survey means that the broadening is now dominated by scattering in essentially all directions. Figure 1 shows contours of constant pulse broadening for the
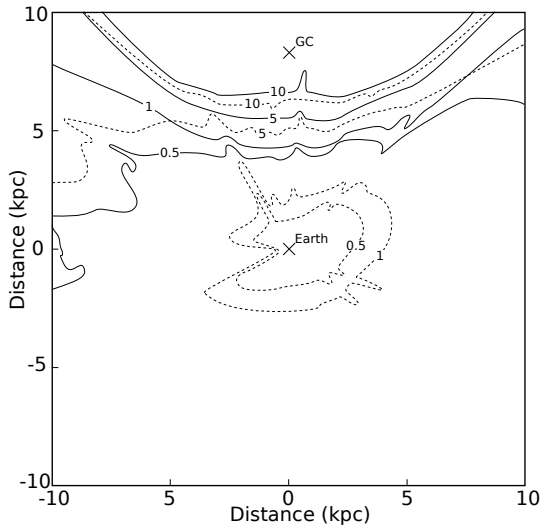
Figure 1. Contours of constant pulse broadening timescale for lines of sight at $b = 0$ for a frequency of 1352 MHz. The values for the PMPS are shown in dashed lines and for the HTRU survey in solid lines, with contours at 0.5, 1, 5 and 10 ms. Scattering timescales and DMs were computed using the model of Cordes & Lazio (2002). The Earth and the approximate location of the Galactic Centre (GC) are shown with crosses.

Table 2. Simulated results for the mean number of total pulsar detections and new discoveries for three previous surveys and the three components of the HTRU survey. The numbers are split the simulation of 'normal' pulsars and 'MSPs' as described in the text. The numbers in parentheses are the actual numbers of pulsars found in each of the complete surveys, where we defined a pulsar as an MSP if it had a period of less than 30 ms and a period derivative less than 10^{-17}.

Survey	Normal		MSPs	
	Total	New	Total	New
PSPS	281 (279)	– (89)	20 (19)	– (17)
PMPS	1008 (1047)	876 (721)	19 (20)	18 (21)
SILS	137 (158)	57 (61)	10 (11)	6 (8)
HTRU				
Low-lat	957	260	51	33
Med-lat	831	52	48	28
High-lat	783	11	65	13

PMPS and HTRU surveys, taking into account both DM and scattering. Even in the worst case, towards the Galactic Centre, the limiting distance of the HTRU survey is greater than twice that of the PMPS, and significantly more in all other directions. This implies that the mid-latitude survey, with an integration time only one quarter that of the PMPS, should still discover pulsars that lie in previously surveyed regions. The deeper low-latitude survey will be able to penetrate further into the Galactic plane for both MSPs and longer period pulsars.

In order to determine the discovery potential of the HTRU survey, we ran simulations of the pulsar population based on the model presented in Lorimer et al. (2006) using the PSRPOP[1] software.

For the normal pulsar population, the input parameters to the model were as follows:

• A log-normal spin period distribution, with mean $10^{2.71}$ ms and sigma $10^{0.34}$ ms.
• A simple power-law for the luminosity distribution, with index -0.59 and low luminosity cut off at 0.1 mJy kpc^2.
• An exponential function for the height above the Galactic plane, with scale 0.33 kpc.
• The radial distribution of Yusifov & Küçük (2004).
• A total of 28000 pulsars, such that the simulated detection of the PMPS matched closely to the true discovery rate.

The number of known Galactic MSPs is small and many previous surveys have been restricted by interstellar dispersion, making simulation of the Galactic population of MSPs more uncertain and indeed this population was not considered by Lorimer et al. (2006). To produce simulations consistent with observed detection rates, we made the following modifications to the model:

• The period distribution was based on that of the known Galactic plane MSPs.
• A larger scale height of 0.5 kpc was used, to better match the known MSP population (Cordes & Chernoff 1997).

Along with the three parts of the HTRU survey, we also simulated the PSPS, PMPS and SILS surveys. The results are summarised in Table 2. In total, the HTRU surveys should discover nearly 400 pulsars, of which 75 will be MSPs, which would represent a doubling of the known population of MSPs. Final results from the survey will also allow us to obtain a better description of the radial and velocity distributions of MSPs.

3 OBSERVING SYSTEM

Observational data are acquired using the Parkes 21-cm Multibeam receiver (Staveley-Smith et al. 1996) and a new digital backend system, the details of which are described in the following sections.

3.1 Analogue systems

The Parkes Multibeam receiver consists of 13 feeds at the prime focus of the Parkes 64 m antenna, organised as a central feed surrounded by two hexagonal rings, with beam pattern on the sky as shown in Figure 2. Our measurement of the system temperature of the central beam – 23 K at 1400 MHz – is slightly higher than the value quoted in Manchester et al. (2001), which may be due to the refurbishment of the analogue electronics in 2006 (J. Reynolds 2010, private communication). The central feed has a symmetric beam pattern, and the feeds further from the prime focus have a slight ellipticity and gain degradation. The details of the receiver and telescope setup are listed in Table 3. For each beam of the receiver, both polarisations are downconverted from 1182-1582 MHz to 0-400 MHz.
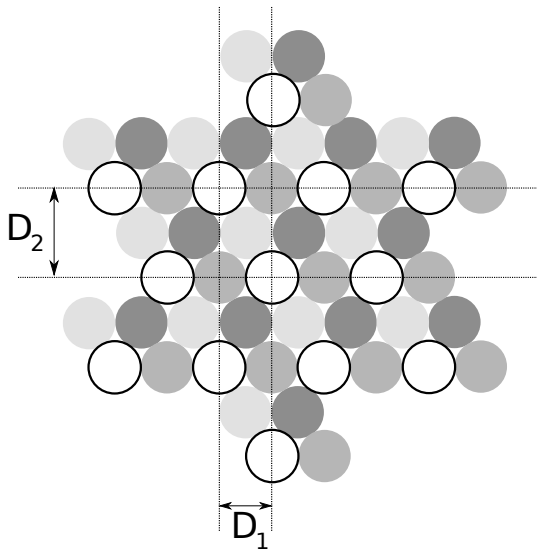
Unfortunately, the high-frequency part of this band is

---

[1] http://psrpop.sourceforge.net

Figure 2. The beam pattern of the Multibeam receiver. The black circles indicate the 14′ FWHM of each of the 13 beams of the receiver. The separation D_1 is also equal to this 14′ FWHM, and $D_2 = \sqrt{3}D_1$ The filled circles show three further pointings interleaved to make up the the shape from which the entire survey is tessellated.

Table 3. Details of the Multibeam receiver for the central feed, the inner ring, and outer ring of feeds, taken from Manchester et al. (2001).

Beam	Centre	Inner	Outer
Telescope Gain (K Jy^{-1})	0.735	0.690	0.581
Half-power beam width (′)	14.0	14.1	14.5
Beam ellipticity	0.0	0.03	0.06
Coma lobe (dB)	none	17	14

badly affected by interference from the Thuraya 3 geostationary communications satellite, which transmits a space-to-earth signal in the 1525-1559 MHz band. We have installed low-pass hardware filters after the receiver that restrict the upper end of our observing band to 1522 MHz; therefore, the effective observing band is 340 MHz wide, centred on 1352 MHz

3.2   The BPSR backend System

The Berkeley-Parkes-Swinburne Recorder (BPSR) system consists of 26 digital spectrometers connected to 13 server-class workstations that format the data and write it to disk. The digital spectrometers are based on the IBOB[2] platform developed by the CASPER[3] group at the University of California, Berkeley, described in detail in McMahon (2008).

Each IBOB consists of two analogue-to-digital converters and two polyphase filters implemented on an FPGA[4].

Each pair samples orthogonal polarisations at 800 MHz using 8 bits per sample, then divides each signal into 1024 spectral channels of width 390 kHz. Each spectral channel is detected and integrated over 25 samples to yield the output time resolution of 64 μs. The 32-bit output of the spectrometer is linearly scaled before decimation to 8 bits; the 8-bit data are written to a single UDP[5] packet with a 2048 byte payload containing 1024 channels times 2 polarisations. Each packet is sent to a 10 Gb/s Ethernet (10GbE) interface connected directly to a Dell PowerEdge 1950 server via a CX4 cable.

On the server, data are collected into 10 s blocks and further processed. Both polarisation streams of each channel are summed and then normalised by subtracting the mean and dividing by the standard deviation (as measured in the first 10 s block of each observation). The resultant data are then decimated to 2 bits per sample and written to disk at a rate of 32 Mb/s.

3.3   Data collection

Each server in the BPSR cluster has sufficient disk space to buffer $\sim$ 3 days of observations. For the HTRU survey, we have chosen to archive the data to magnetic tapes before removing the data from the buffer, allowing for continuous observing. One copy is written to tape at Parkes and another is streamed via a dedicated 1 Gb/s fibre link to the supercomputer located at Swinburne University. Here the data are also written to magnetic tape and, if there is sufficient free capacity on the supercomputer, run through the survey data processing pipeline in close to real-time.

In addition to the astronomical signal, the BPSR backend also records a header file and a collection of auxiliary data files for each beam. The header file contains information about the observation in an XML[6] format as described in Section 3.4. The auxiliary files contain bandpass and low resolution time series snapshots, as described in Section 3.5. The raw time series is stored in the SIGPROC[7] 'filterbank' data format, which consists of a binary header followed by continuous raw data.

For the HTRU survey, all data are recorded using two bits of precision and with four samples packed per byte, with the first sample in the lowest significant bits of the byte. The data are ordered first by frequency then by time, each time sample being stored as a consecutive 256 byte word. The raw data are preceded by a 345 byte header, used for backwards compatibility with the SIGPROC software, however more information is available in the XML header file. These data are then packed with the header and auxiliary files into a single GNU tarball per beam.

3.4   Psrxml header format

The psrxml header is a format-independent XML header file that describes both the observational properties of the recorded data and the format of the actual data itself. The

---

[2] Internet Break-Out Board
[3] Center for Astronomy Signal Processing and Electronics Research
[4] Field Programmable Gate Array
[5] User Datagram Protocol
[6] eXtensable Markup Language, http://w3.org/TR/REC-xml/
[7] http://sigproc.sourceforge.net

psrxml header file is stored separately to the raw data, allowing trivial indexing of header data for very large data files, such as those produced by the BPSR backend.

The psrxml data format is intended to be suitable for long term archival of pulsar data for future uses. Features of note are:

• Checksumming of data blocks: As the data are written to disk, each block of data (usually a few hundred megabytes) is passed through the SHA-1[8] hash algorithm and the hash value stored in the header file. This allows for the data to be checked for errors and consistency at a later time. Archival data are valuable: This check-summing ensures that data extracted from an archive are identical with the data recorded at the telescope.

• Format and machine independence. The psrxml header file is written in a well-defined format, typically encoded in standard 7-bit ASCII[9]. This means that the header will be readable on almost any computer that exists or is likely to exist. Since the header completely describes the data format, in terms of bit and byte ordering, and which bytes to read, one can therefore read the raw data on any computer with the appropriate software.

• Human readable. XML documents can be easily read using a standard text editor. With the use of XSL[10], viewing a psrxml header file in a web browser displays the data in a pleasant format without the use of any specialist software. This does not change the file in any way, so the file is readable in ideal formats by both machine and human.

• Extendable. Since the header is written in XML, it is trivial to add new XML tags to the file in a safe manner, storing either fields specific to a certain project, or extending the data format to new generic uses.

3.5 Auxiliary files

In addition to the header and data files, data generated for on-line monitoring of the system are stored for future use. This consists of the passband and time series measured in the pre-normalised, dual-polarisation, 8-bit data samples, completely averaged in frequency.

3.6 Data tracking

At the completion of every observation, a copy of the psrxml header file is kept on disk and indexed in a book keeping database. The database links the observation against the planned observations and marks that observation as completed, removing that pointing from the pool of pointings from which observing schedules are selected.

[8] Secure Hash Standard, Federal Information Processing Standards Publications, 180-1, 1995
[9] American Standard Code for Information Interchange, American National Standards Institute, X3.4-1986, 1986
[10] eXtensable Stylesheet Language

4 PROCESSING

Processing of the survey is currently being carried out at the Jodrell Bank Centre for Astrophysics and the Swinburne Centre for Astrophysics and Supercomputing.

The analysis of our data is limited by the available computational power, therefore re-processing of the data with future computer hardware will likely yield additional results. We follow a typical pulsar search workflow as described, for example, in Lorimer & Kramer (2005).

4.1 Software Pipeline

For our survey processing we have developed the HITRUN processing pipeline. HITRUN is designed to be a flexible system that can process both BPSR data and legacy 1-bit data formats without modifying the software. This flexibility, as well as being a useful tool, allows us to easily test the software on legacy data and against legacy codes.

The HITRUN pipeline is composed of several stages: Radio frequency interference (RFI) removal, dedispersion, time series analysis, candidate sorting, candidate folding and optimisation. Here, we outline the algorithms used for each step of the process.

4.1.1 RFI removal

RFI removal consists of two tasks, removal of 'bad' spectral channels, and removal of 'bad' time samples.

First, we remove spectral channels that are affected by periodic RFI. Initially, we have a list of channels that are known to have poor data quality, and these are always removed. Then, we Fourier analyse each of the channels individually, using the Fourier time series analysis described below. If any signals are detected with a signal-to-noise ratio (SNR) of greater than 15, we reject that channel.

Next, we sum the data in frequency, producing a single time series at DM = 0. This time series is then searched for bursts of emission, and if found, those samples are removed from the time series. To remove longer duration RFI bursts, we sum together 2, 4, 8 16 and 32 adjacent samples and repeat the search. Any time samples that are removed in this process are then removed from the original data file, replaced by samples that are drawn from a random population statistically indistinguishable from the data. An example of this RFI removal is shown in Figure 3, where a series of short-duration wide-band signals have been removed from the data. It should be noted that this process will remove low-DM astrophysical signals of sufficient intensity and width. With our 5-σ threshold for removal, astrophysical signals of maximum recordable intensity will be removed if their DM is less than $0.12(W/64\mu s)$ cm^{-3}pc, where W is the approximate width of the pulse.

4.1.2 Dedispersion

Since the DM of any signal is not known a priori, we have to search many trial DM values. We must therefore transform the single time series with many frequency channels into many frequency-summed time series with different dispersion delays. For our survey, the processing time is largely
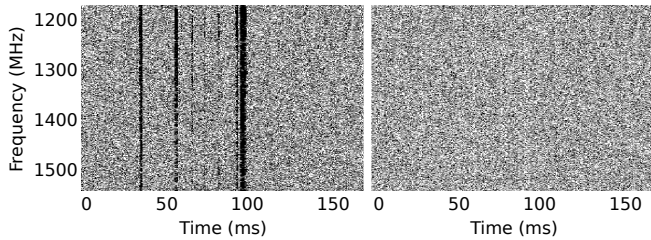
Figure 3. The intensity of recorded signals over a short time as a function of frequency, before (left) and after (right) RFI removal. The RFI can be seen as a series of vertical stripes, which are replaced with random noise by the RFI excision routine.

dominated by the dedispersion time, making it important to choose the most efficient algorithm possible.

The most efficient dedispersion algorithm known is the 'tree' dedispersion approximation of Taylor (1974). This, however, assumes a linear dependence of delay on frequency, which is a good approximation for small fractional bandwidths. For many recent surveys with large fractional bandwidths this approximation is inappropriate, and work-arounds have been used. In the PSPS, a two-step approach was used where smaller sub-bands were dedispersed using the tree algorithm, before a final dedispersion step to combine the sub-bands (Manchester et al. 1996). In addition to this, the PMPS used a linearisation approach where the data were padded with empty channels in a manner such that the dispersion sweep could be considered linear Manchester et al. (2001). For the HTRU survey we have decided not to use the tree algorithm as the cost of linearising the data outweighed the gain from the more efficient algorithm. Instead, we have chosen to implement an efficient ν^{-2} dedispersion algorithm.

Much of the cost of dedispersion is due to the large volume of data that must pass through the system, therefore we compact the data as much as possible. Since we sum 1024 2-bit values per output sample, there are 4096 possible output levels. Our processing systems perform 64-bit integer arithmetic, so we can pack 4 samples per 64-bit word, giving a factor of 4 processing throughput increase. By dividing the output by 16, the number of levels is reduced to 256, with little sensitivity loss. We therefore only need to write out 8-bits per sample, keeping the input/output costs to a minimum. Additionally, we make use of modern multi-core processors with multi-threaded code performing 4 dedispersion threads simultaneously. In future, it will likely be possible to gain additional performance benefits with technologies such as graphics processing unit co-processing.

4.1.3 Time series analysis

By this stage of the processing we have a number of dedispersed time series on disk, which have to be searched for pulsar signals. HITRUN provides both time-domain and frequency-domain methods.

In the frequency domain we take the power spectrum of the data using a fast Fourier transform. We then remove the strong red-noise component of the spectrum at frequencies below about 10 Hz by subtraction of a running mean and division by a running variance. This also has the effect of normalising the spectrum. The resulting power spectrum is then searched for signals with a signal-to-noise ratio of greater than 6. To reclaim power in the harmonics of narrow pulses, we also search spectra which have had 2, 4, 8 and 16 harmonics summed. Potential signals from each DM trial are written out for later sorting, as described below.

In the time-domain we conduct a search with similar methodology to that reported in Burke-Spolaor & Bailes (2010). In brief, we search for bright, single pulses by collating all points above 6-σ from the mean, after which the detections from a single pointing are compared across all the beams to identify sky-localised events. Details of the single-pulse-specific analysis and the results of the time-domain search will be reported in a future paper.

4.1.4 Candidate sorting

Candidate sorting is the process of collecting the Fourier detections from each DM step and combining those into a manageable number of candidate pulsars for further analysis. This is done by grouping detections with the same frequency into a single candidate, and by combining candidates that are harmonically related. In HITRUN, this is done using software from PULSARHUNTER[11].

4.1.5 Candidate folding and optimisation

We then fold the data, producing an averaged pulse profile for each candidate. Folding is a coherent technique unlike the incoherent harmonic summing in the Fourier domain. HITRUN utilises the DSPSR[12] software to fold each candidate, producing profiles for each of 16 frequency bands and 32 sub-integrations.

Then the PSRCHIVE package (Hotan et al. 2004) is used to sum the folded sub-integrations and periods with a series of trial periods and DMs around the values returned from the Fourier domain search. The optimised period and DM, i.e. that which give highest folded SNR, are then used to make the final diagnostic plots for the candidate.

4.2 Selection of candidates

The goal of the data processing is to select a number of likely pulsar signals for re-observation. To achieve this, we take the optimised candidates and the associated diagnostic plots and view them with graphical candidate selection tools, such as JREAPER (Keith et al. 2009). These tools reduce the large number of candidates to a series of points on a scatter chart, usually with period and SNR on the axes. Selecting these points presents the user with the full candidate details and diagnostic plots, at which point the user must exercise judgement on whether the candidate should be flagged for further follow up.

Since manual candidate selection is a time consuming and potentially error prone process, we are investigating the potential for using artificial neural network (ANN) algorithms to pre-select promising candidates for viewing (Eatough et al. 2010). An ANN is a mathematical construct,

---

[11] http://www.pulsarastronomy.net/wiki/Software/PulsarHunter
[12] http://dspsr.sourceforge.net

consisting of a set of nodes that are connected to form a decision tree that, based on a given input vector, derives a conclusion about the validity of a hypothesis. In our case, we provide the ANN with a vector of 'scores', formed from analysis of the diagnostic plots, e.g. the agreement of the observed SNR-DM curve of a candidate with theoretical predictions as measured by a χ^2 estimator. The more types of scores that are used, the larger (usually) the chance to differentiate between pulsar and non-pulsar signals, however the more known pulsar signals are required to 'train' the ANN (Eatough et al. 2010). Indeed, our ANN is poor at selecting binary or millisecond pulsars, because of the limited size of training set available for these classes of pulsar. The effectiveness of this technique can be seen in the discovery of PSR J1701–44, which was identified as a candidate by the ANN. The SNR of the candidate was rather low, at only 7, and would quite probably have been missed by a graphical interface reliant upon a human to select the candidate manually.

Although the ANN is limited in the types of pulsars it will select, it does provide a thorough analysis of all the candidates free from human error. We find that adding the ANN to our existing candidate selection effort gives a beneficial additional way to select candidates, with little cost in terms of required computing power. Direct inspection of candidates is vital, however, and remains the primary way that pulsars have been discovered in the HTRU survey.

5 SURVEY SENSITIVITY

Knowledge of the minimum detectable flux density of the survey is vital for determining the survey effectiveness. Determining this limiting flux density is not trivial, since the survey is not uniformly sensitive, even over a small region of sky, nor to all pulsars. One option is to compute a theoretical mean sensitivity to some standard 'typical' pulsar, as done by other large pulsar surveys. This gives a value that can be easily compared to other similar surveys.

To measure the actual sensitivity of the survey, we can look at re-detections of known pulsars. Since published values exist for the position and flux density of thousands of pulsars, we can cross match those positions with our survey pointings. We then compute the theoretical SNR value for that pulsar given the offset in the beam position and compare that to the output of the search pipeline. We consider each of these in in turn below.

5.1 Theoretical sensitivity

The radiometer equation can be used to compute the fundamental limiting flux density for the centre of the central beam of a given survey observation.

$$S_{\min} = \frac{\sigma(T_{\mathrm{sys}} + T_{\mathrm{sky}})}{G\sqrt{2B\tau_{\mathrm{obs}}}}, \tag{1}$$

where σ is the minimum acceptable SNR, T_{sys} is the system noise temperature, T_{sky} the sky noise temperature, G is the system gain, B is the observing bandwidth and τ_{obs} is the integration time. T_{sky} is only a significant contribution to the system noise for low Galactic latitudes and has a strong dependence on the area of sky that is observed. The value of

Table 4. The maximum, minimum and mean sky noise temperature over the three survey regions. Note that the values for the mid-latitude survey exclude the low-latitude survey region.

Survey	Mean (K)	Max (K)	Min (K)
Low	7.6	36.0	1.6
Mid	2.5	9.1	0.6
High	1.0	2.4	0.6

T_{sky} at 1352 MHz for the survey region is extrapolated from the Haslam et al. (1981) sky map at 408 MHz. For Equation 1 we use the mean values listed in Table 4, however it should be noted that T_{sky}, and therefore $S_{\min}$, varies considerably across the sky. Here we use $\sigma = 8$, $T_{\mathrm{sys}} = 23$ K and $G = 0.735$ to compute a $S_{\min}$ of 0.20, 0.47 and 0.61 mJy for the low, mid and high latitude portions of the survey respectively. However as described below, the practical limiting flux density is lower due to the narrow pulse width of most pulsars.

Our Fourier based detection algorithm is not uniformly sensitive to all DMs, pulse periods and pulse shapes. This is somewhat difficult to quantify, however we follow the approach of Manchester et al. (2001) by modelling the frequency response of the pulsar as a uniform train of impulses separated by frequency $f_p = 1/P$. This train of pulses has amplitude $1/S_{\min}$, to which we multiply a series of functions representing the various transformations that the data undertake.

We can model each pulse as a Gaussian with width $W_{50} = 0.05P$, so that the frequency response is multiplied by the Gaussian

$$F(f) = \exp\left(-\frac{(\pi f W_{50})^2}{4\ln(2)}\right). \tag{2}$$

The pulses are also convolved with the effect of interstellar dispersion, which can be modelled as another Gaussian with width τ_{DM}, the dispersion delay. Finally we must account for the finite sampling interval, τ_s, which multiplies the amplitudes by

$$F(f) = \left|\frac{\sin(\pi f \tau_s)}{\pi f \tau_s}\right|. \tag{3}$$

The final SNR is computed after summing N harmonics, where $N \in \{1, 2, 4, 8, 16\}$. Figure 4 shows the minimum detectable flux density as a function of pulsar period and DM for the mid-latitude survey. It can be seen that the HTRU survey is sensitive to MSPs out to DMs of a few hundred cm^{-3}pc. The effects of T_{sky} and the differing observing time for the three surveys can be seen in Figure 5, which shows the sensitivity curves for the three surveys at the minimum and maximum T_{sky} in that survey region.

The mean sensitivity of the survey is reduced by a number of factors. Firstly, the outer beams of the receiver are less sensitive than the centre beam, and the sensitivity of each beam reduces towards the edges. This means that the sky coverage is not uniform, with the mean sensitivity over the mid-latitude survey of about 0.25 mJy.
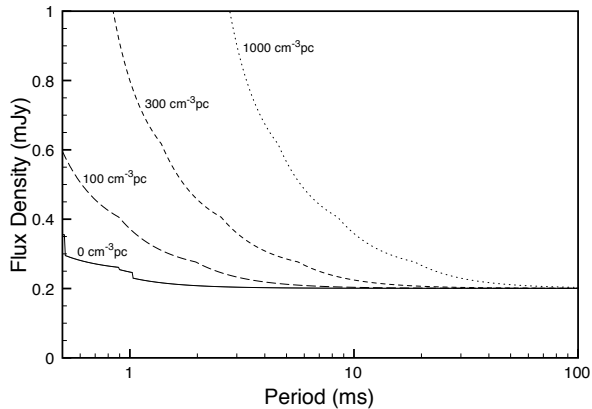
Figure 4. The mean limiting flux density for the mid-latitude survey shown as a function of pulsar period for various values of DM. Values shown here assume a pulse duty cycle of 5%.
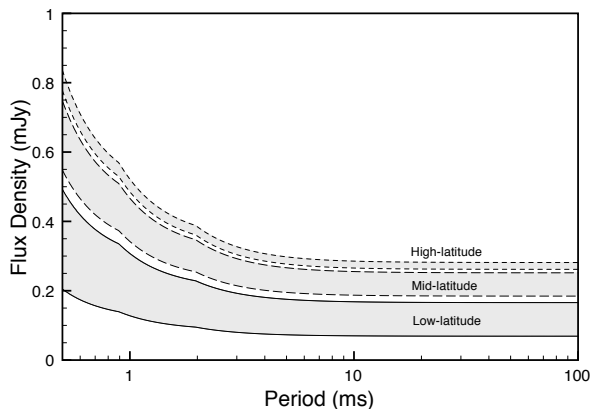

Figure 5. Comparison of the sensitivity of the three survey regions for a pulsar with a DM of 100 cm^{-3}pc. Each region has two curves, showing the values for the minimum and maximum value of $T_{\rm sky}$ in the survey region.

5.2   Re-detection of known pulsars

A total of 290 previously known pulsars lie within one beamwidth of one of the HTRU survey pointings collected to date. For each pulsar we obtained the flux density and its error from the pulsar catalogue[13], a value of $T_{\rm sky}$ at the pulsar position, and the offset between its position and the centre of the relevant beam. We then computed the expected SNR for each pulsar following the process outlined in Section 5.1.

In all, we detected 223 of the 290 pulsars. For the 67 pulsars we failed to detect, 5 observations were ruined by broad-band RFI, 54 pulsars were not detected above a SNR of 10 even after we folded observations at the known pulsar ephemeris. This leaves 8 pulsars that are seen in folded observations with a SNR of greater than 10 but were not detected in our search procedure. Each of the the 8 pulsars had a spin period above 500 ms, and so the Fourier SNR may well have been reduced by a larger red-noise component in the data, or the pulsar period falling between Fourier bins.
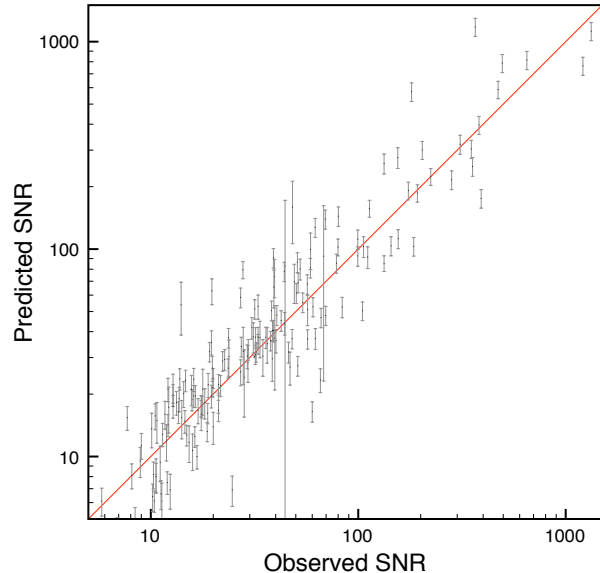
Figure 6. The predicted SNR for 223 known pulsars re-detected in the HTRU survey, shown as a function of the observed SNR. Errors shown are from the published error in the pulsar flux density. The line shows the expected 1:1 correlation.

The loss of pulsar detections due to RFI is an uncontrollable aspect of search observations. Although we have applied the techniques described in Section 4.1.1, they are unable to remove this type of broad-band RFI. Future re-processing using the technique of Eatough et al. (2009) may be possible, however this is currently unfeasible as it would increase the time for processing the survey data by more than a factor of ten.

Figure 6 shows the expected versus actual SNR for the 223 detected pulsars. Although the correlation between the predicted and observed values is good, the predicted values are, on average, somewhat higher than the observed values. This can be caused by either sensitivity loss in our observing system, or error in the catalogued flux densities. First, we checked that the backend was not introducing any loss by collecting data simultaneously with BPSR and the Parkes Digital Filterbank 3 (PDFB3). These observations show that the BPSR and PDFB3 performance are equivalent and we therefore consider it unlikely that the backend is introducing any losses. Hobbs (private communication), has shown that the catalogue flux densities appear to be systematically higher than those obtained in interferometric observations. This bias may be due to the tendency to publish only the data with the highest SNR, for example when scintillation boosts the apparent flux density. Given our ability to detect the majority of the pulsars that are in our search area, we are relatively confident that the system is performing to specification.

6   NEW PULSAR DISCOVERIES

In this paper we present the results of the analysis of the first $\sim 30\%$ of the mid-latitude part of the survey. Results so far include:

Table 5. Basic parameters for the 27 pulsars discovered in the HTRU survey to date. Pulsars for which no full timing solution is published have been assigned a temporary name containing only two digits of declination.

PSR J	l (°)	b (°)	Period (s)	DM (cm^{-3}pc)
1125−58[1]	291.8	2.6	0.003102	125
1330−52	308.8	9.6	0.648104	149
1433−50	318.9	9.1	1.017495	98
1442−51	320.1	7.7	0.732061	97
1517−46	327.38	9.22	0.88661	139
1612−58	327.0	−5.0	0.615520	172
1623−4950[2]	333.9	−0.1	4.325800	881
1625−49	334.6	0.0	0.355856	717
1627−59	327.3	−7.3	0.354239	92
1648−36	347.1	5.8	0.212316	222
1650−60	328.2	−10.2	0.583771	106
1701−44	342.3	−1.3	0.755535	413
1705−43	343.3	−1.5	0.222561	184
1705−61	328.7	−12.2	0.808546	87
1708−35[1]	350.4	3.2	0.004505	146
1731−18[1]	6.9	8.2	0.002345	106
1753−38	352.3	−6.4	0.666804	168
1754−24	4.9	0.8	2.090263	789
1801−32[1]	358.9	−4.5	0.007454	177
1802−33	357.6	−5.5	2.461052	254
1803−33	358.0	−5.6	0.633412	171
1810−01	27.0	8.6	0.744976	135
1811−24[1]	7.1	−2.5	0.002661	60
1811−49	344.2	−14.2	1.432704	49
1812−27	4.0	−4.6	0.236983	105
1814−05	23.8	5.8	1.014405	119
1854−15	19.0	−8.0	3.453121	157

[1] Timing parameters in Bates et al. (in prep).
[2] Timing parameters in Levin et al. (2010).

• Discovery of 5 MSPs, all of which are in binary systems. Full details of these pulsars will be reported in Bates et al. (in prep).
• Discovery of the radio pulsar with the highest known magnetic field which appears to be a radio-loud magnetar, as reported in Levin et al. (2010).
• Discovery of 21 pulsars with periods between 0.2 and 3.5 s and moderate to high DMs. These are likely 'standard' solitary radio pulsars but full timing solutions still need to be obtained.

The Galactic coordinates, spin period and DM for each of these pulsars is given in Table 5.

6.1 Comparison to PMPS

Figure 7 shows a comparison between the sensitivities of the mid-latitude and low-latitude HTRU survey and the PMPS for a DM of 100 cm^{-3}pc. Although the mid-latitude HTRU survey has only one quarter the observing time of the PMPS, it is significantly more sensitive to short period pulsars at
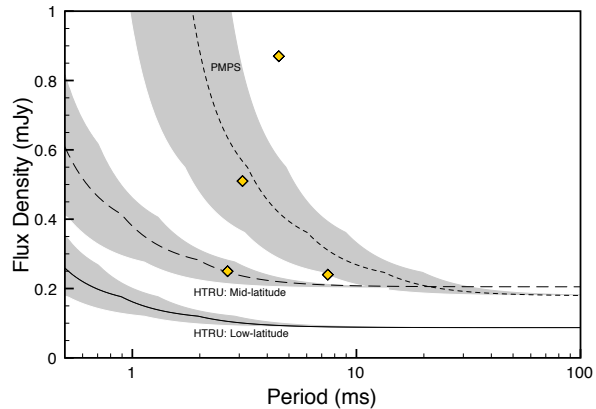

Figure 7. Comparison of the Mid and Low latitude parts of the HTRU survey and the PMPS. The lines give the sensitivity limit for a DM of 100 cm^{-3}pc. The shaded areas show the range of sensitivities for DMs between 50 and 150 cm^{-3}pc. Note that the limiting flux density for the Mid-latitude survey used for this curve is computed using the mean T_{sky} for the PMPS survey area. Also shown as diamonds, are the periods and estimated flux densities for the four MSPs discovered in HTRU survey that lie in the PMPS region.

large DMs. This is due to a combination of the faster sampling rate, narrower frequency channels, slightly increased total bandwidth and multi-bit sampling of our survey.

Of the new discoveries, 9 pulsars lie within the sky coverage of the PMPS. We have re-analysed archival data for each of these pulsars and the results are presented in Table 6. Four of these pulsars are MSPs with high DMs and are included on Figure 7. It can be seen that all bar one fall below the (nominal) PMPS detection threshold. In fact, re-examination of the PMPS archival data shows that both PSR J1708–35 and J1801–32 are visible but that the pulse broadening from the 3 MHz channel bandwidth makes them difficult to distinguish from sinusoidal interference in a blind search.

Of the remaining five pulsars, three are seen in the archival data with low SNR and none were selected for re-observation in the PMPS. Although the pulsar positions are not well known at this time, the nominal position of each falls more than 5 arc-minutes from the beam centre of the PMPS observation. Therefore we suggest that these pulsars fall in the regions between beam centres where the PMPS sensitivity is lowest. Two pulsars appear to be below the detection limit of the PMPS including the newly discovered magnetar PSR J1622–4950, which shows extreme time variability (Levin et al. 2010).

7 CONCLUSION

We have described the system configuration and initial discoveries of a new pulsar survey using the Parkes radio telescope. At the time of writing, a total of 250 pulsars have been detected, of which 27 are new discoveries. The high time and frequency resolution of our digital backend system leads to increased sensitivity to short-period, high-DM pulsars compared to previous surveys. Indeed, 5 of our new

Table 6. Pulsars discovered in the HTRU survey for which archival data exists in the PMPS at the position of the pulsar. The unique PMPS grid identification number (see Manchester et al. 2001 for details) for the processed beam, the MJD of the observation and the SNR and periodicity if the pulsar was detected.

PSR J	Grid ID	MJD	SNR	Period (s)
1125−58	G4707513	51296.42	--	--
1622−4950	G4887499	50686.25	--	--
1625−49	G4891500	50686.23	7.9	0.3558530
1701−44	G4924493	51152.94	6.4	0.7555360
1705−43	G4928493	51457.10	10.4	0.2225614
1708−35	G4959516	51718.68	17.4	0.0045052
1754−24	G5021504	50843.07	--	--
1801−32	G4995477	52080.69	14.4	0.0075344
1811−24	G5030488	51245.84	--	--

discoveries are MSPs at high DM, all of which lie within previously surveyed regions of sky.

8   ACKNOWLEDGEMENTS

REFERENCES

Archibald A. M. et al., 2009, Science, 324, 1411
Burgay M. et al., 2003, Nature, 426, 531
Burke-Spolaor S., Bailes M., 2010, MNRAS, 402, 855
Cordes J. M., Chernoff D. F., 1997, ApJ, 482, 971
Cordes J. M., Lazio T. J. W., preprint (arXiv:astro-ph/0207156)
Eatough R. P., Keane E. F., Lyne A. G., 2009, MNRAS, 395, 410
Eatough R. P., Molkenthin N., Kramer M., Noutsos A., Keith M. J., Stappers B. W., Lyne A. G., 2010, MNRAS, submitted
Edwards R. T., Bailes M., van Straten W., Britton M. C., 2001, MNRAS, 326, 358
Haslam C. G. T., Klein U., Salter C. J., Stoffel H., Wilson W. E., Cleary M. N., Cooke D. J., Thomasson P., 1981, A&A, 100, 209
Hessels J. W. T., Ransom S. M., Stairs I. H., Freire P. C. C., Kaspi V. M., Camilo F., 2006, Science, 311, 1901
Hewish A., Bell S. J., Pilkington J. D. H., Scott P. F., Collins R. A., 1968, Nature, 217, 709
Hobbs G. B. et al., 2009, Publ. Astr. Soc. Aust., 26, 103
Hotan A. W., van Straten W., Manchester R. N., 2004, Proc. Astr. Soc. Aust., 21, 302
Jacoby B. A., Bailes M., Ord S. M., Edwards R. T., Kulkarni S. R., 2009, ApJ, 699, 2009
Keith M. J., Eatough R. P., Lyne A. G., Kramer M., Possenti A., Camilo F., Manchester R. N., 2009, MNRAS, 395, 837
Keith M. J., Johnston S., Kramer M., Weltevrede P., Watters K. P., Stappers B. W., 2008, MNRAS, 389, 1881
Kramer M. et al., 2006, Science, 314, 97
Levin L. et al., 2010, Science, submitted
Lorimer D. R., Bailes M., McLaughlin M. A., Narkevic D. J., Crawford F., 2007, Science, 318, 777
Lorimer D. R. et al., 2006, MNRAS, 372, 777
Lorimer D. R., Kramer M., 2005, Handbook of Pulsar Astronomy. Cambridge University Press
Lyne A. G. et al., 2004, Science, 303, 1153
Lyne A. G. et al., 1998, MNRAS, 295, 743
Manchester R. N. et al., 2001, MNRAS, 328, 17
Manchester R. N. et al., 1996, MNRAS, 279, 1235
McLaughlin M. A. et al., 2006, Nature, 439, 817
McMahon P., 2008, Master's thesis, University of Cape Town
Staveley-Smith L. et al., 1996, Proc. Astr. Soc. Aust., 13, 243
Taylor J. H., 1974, A&AS, 15, 367
Verbiest J. P. W. et al., 2009, MNRAS, 400, 951
Weltevrede P. et al., 2010, ApJ, 708, 1426
Yusifov I., Küçük I., 2004, A&A, 422, 545